HiLL PUBLISHING

Journal of Applied Mathematics and Computation, 2023, 7(2), 288-297
https://www.hillpublisher.com/journals/JAMC/
ISSN Online: 2576-0653
ISSN Print: 2576-0645

Transmission Loss Performance Analysis of Acoustic Coatings under Hydrostatic Pressure Considering Cavity Pressure

Shuailong Zhou, Ni Yu*, Hongbo Tao, Fenghui Kang

Luoyang Ship Material Research Institute, Luoyang, Henan, China.

How to cite this paper: Shuailong Zhou, Ni Yu, Hongbo Tao, Fenghui Kang. (2023) Transmission Loss Performance Analysis of Acoustic Coatings under Hydrostatic Pressure Considering Cavity Pressure. *Journal of Applied Mathematics and Computation*, 7(2), 288-297.
DOI: 10.26855/jamc.2023.06.010

Received: June 3, 2023
Accepted: June 29, 2023
Published: July 30, 2023

***Corresponding author:** Ni Yu, Luoyang Ship Material Research Institute, Luoyang, Henan, China.

Abstract

Underwater acoustic coatings laid on the hull surface of underwater vehicles is squeezed under the action of high hydrostatic pressure, changing its shape and material parameters, which has a great impact on sound performance. Therefore, studying the sound performance of underwater acoustic coatings under high hydrostatic pressure is great significance for the stealth performance of underwater vehicles. Considering the effect of pressure inside the cavity on the structure deformation and acoustic properties under static pressure, the single-cell deformation of the acoustic coatings containing the cavity is calculated based on axisymmetric finite element simulation. The shape variables are introduced into the two-dimensional theoretical model of the acoustic coatings and the theoretical transmission loss (TL) curve of the coatings is obtained. A comparative analysis of acoustic-solid coupling is carried out using the deformed geometric model to verify the effectiveness of both theoretical analysis and numerical simulation methods for solving TL. The theoretical validity of this paper was verified by experimental comparison. The results show that, without considering the material parameter changes, the acoustic coatings under static pressure undergoes single-cell axial and cavity radial shrinkage, and the sound insulation performance gradually decays, not only that, the cavity pressure resists the shrinkage under static pressure, while attenuating the tendency of curve decay. The results of the study have some reference for forecasting the sound performance of acoustic coatings under static pressure.

Keywords

Transmission loss, Static pressure, Theoretical analysis, Cavity pressure

1. Introduction

To reduce the acoustic scattering from underwater targets, the application of acoustic coatings on the surface of underwater vehicles is one of the most common methods. A typical underwater cover consists of a rubber matrix and an internal cavity, which is limited by the operating environment and the structure will be deformed to varying degrees with changes in operating pressure. The air inside the cavity will be compressed, further affecting the acoustic characteristics of the structure. Therefore, it is important to carry out theoretical research on the acoustic properties of acoustic coverings under static pressure.

At present, more achievements have been made in the research on acoustic coatings containing cavities. Gaunaurd [1] proposed a one-dimensional analysis method for viscoelastic media with short cylindrical cavities, which physically explains the acoustic properties of the coatings according to the resonance of different physical dimensions and modes of

the cavities. Beili Zhu [2] used elastic wave propagation theory to transform the model of rubber media containing cylindrical cavities into a homogeneous material layer with equivalent wave number, and then combined with the transfer matrix method [3] to solve the acoustic coefficients of the overall acoustic coatings. Wenwen Jiang et al. [4] applied the finite element method to calculate the deformation of rubber acoustic structure and its acoustic performance under static pressure. The results showed that the acoustic band of several typical cavity structures moved toward high frequencies as the static pressure increased, which was consistent with the change trend of the measured results. Huang Xiu-Chang et al. [5-6] established a method to measure the dynamic mechanical parameters of rubber materials under static pressure using hydroacoustic sound tubes.

In this work, we propose to model the finite element model after exporting the pressurized finite element model and then reassigning the material parameters to consider the effect of cavity pressure on the performance of underwater acoustic coatings to eliminate the errors due to geometric approximation. The effects on TL are compared under the consideration of cavity pressure to reveal the pattern of influence of cavity pressure on the acoustic properties of the coatings.

2. Theoretical model

2.1 Model analysis

This investigation will focus on the acoustic effect of the cavity-containing coatings at depths up to 300m in seawater. Since rubber has the characteristics of small Young's modulus and large Poisson's ratio, its susceptibility to extrusion deformation under hydrostatic pressure is no longer negligible [4]. The deformation behavior of rubber containing cavity under hydrostatic pressure is quite complex, at this time, the model to characterize the deformation behavior of cavity rubber according to material properties includes wired elasticity, hype elasticity and other models. At present, the finite element method is mainly used to calculate the rubber deformation under static pressure, that is, the static material parameters are substituted into the finite element software to solve for the deformation. For the calculation of sound propagation, due to the special characteristics of rubber materials, the Young's modulus, Poisson's ratio, and loss factor of rubber materials under acoustic excitation of different frequencies are different, so dynamic material parameters must be used to calculate the sound absorption coefficient of rubber materials under acoustic excitation.

Based on the above conditions, the procedure of analysis in this investigation is shown in Fig 1:

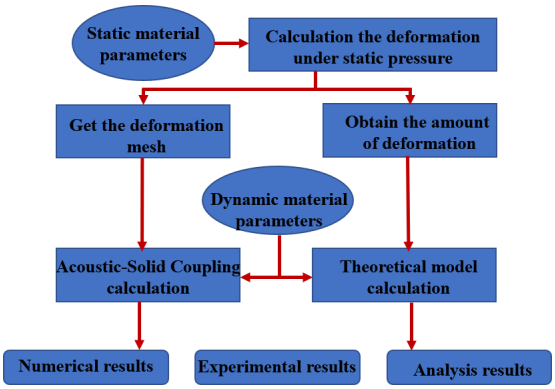

Figure 1. Flowchart of TL calculation for acoustic coatings under hydrostatic pressure.

2.2 Mathematical model

Figure 2 shows a uniform cylindrical tube with a length of d with a cavity diameter of r_b and an outer diameter of r_a. It can be regarded as a section with cavity acoustic coatings. In particular, the radial displacement of the outer wall of the cavity is constrained and the inner wall is free.

The equivalent complex wavenumber of a cylindrical cavity in a rubber matrix can be expressed as [7]:

$$k_z^2 = \frac{1}{1+3\varepsilon^2}\left(1+\frac{\lambda}{\mu}\varepsilon^2\right)k_l^2 \tag{1}$$

Where, ε is the aperture ratio of the cavity; k_l, λ, μ are the longitudinal wave number and the Lame constant of uniform rubber, respectively.

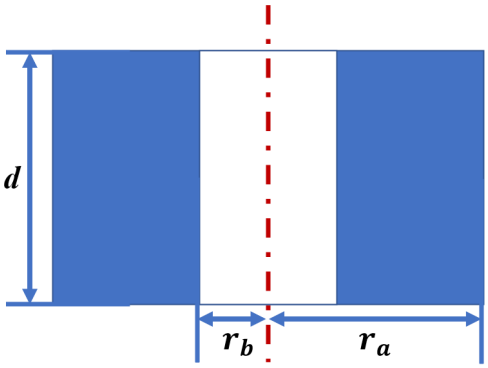

Figure 2. Illustration of uniform cylindrical cavity section.

First, the equivalent complex wave number and density of the cylindrical cavity are calculated. The axisymmetric cavity is divided into multiple segments, each segment can be approximated as a cylindrical tube, and the equivalent complex wave number and density of each segment can be further obtained. The sound propagation state of a cavity cylinder is equivalent to that of an infinite multi-layer uniform medium, which is constrained by the radial displacement of the uniform cylinder. The transfer matrix method is applied to obtain the reflection coefficient at the incident end and the transmission coefficient through the coatings, as shown in Fig 3. As shown in the figure: p_{in} is the incident pressure;p_r is the reflection pressure; p_t is transmission pressure; ρ_i is the density of the i-th layer; k_{iz} is the equivalent axial wavenumber of layer i; ε_i is the aperture of layer i; d_i is the thickness of layer i,i= 1,2,…, n; $p_z^{(n+1)}$ is the sound pressure of the outgoing end; $v_z^{(n+1)}$ is the normal vibration velocity of the exit end surface; Z_0 is the incoming end characteristic impedance; Z_{n+1} is the outgoing end characteristic impedance.

The process is shown in Fig 3(a), which is equivalent to a multi-layer homogeneous structure and then using the transfer matrix method to solve the acoustic propagation coefficient is as shown in Fig 3(b). The calculation formula of relevant parameters is as follows [7, 8]:

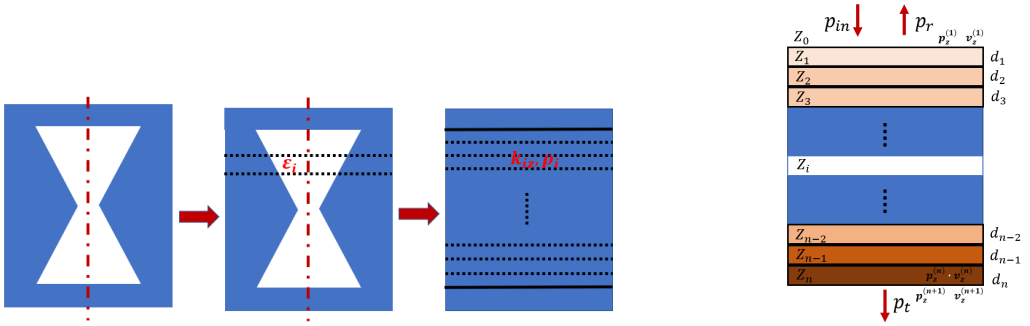

(a) The gradient cavity is equivalent to a multi-layer medium (b) Schematic diagram of transfer matrix method

Figure 3. Illustration of transition cavity equivalent to multilayer medium and transfer matrix method.

$$\begin{aligned} k_{iz}^2 &= \frac{1}{1+3\varepsilon_i^2}(1+\frac{\lambda}{\mu}\varepsilon_i^2)k_1^2 \\ c_i &= 2\pi f/k_{iz} \\ \rho_i &= (1-\varepsilon_i^2)\rho_{\text{rubber}} + \varepsilon_i^2\rho_{\text{air}} \\ \varepsilon_i &= r_{\text{b}i}/r_a \end{aligned} \tag{2}$$

Where: ρ_{rubber} is the uniform rubber density; ρ_{air} is the air density; f is the incident wave frequency; r_{bi} is the inner diameter of the cavity in layer i; c_i is the equivalent sound velocity in layer i.

In the case of perpendicular incidence of sound waves, the acoustics coatings with multiple sound pressure and normal velocity transfer relationship between two adjacent layers of the media is as follows [9, 10]:

$$\begin{Bmatrix} p_z^{(i)} \\ v_z^{(i)} \end{Bmatrix} = \begin{bmatrix} \cos k_{iz}d_i & \text{j}Z_i\sin k_{iz}d_i \\ \text{j}\sin k_{iz}d_i/Z_i & \cos k_{iz}d_i \end{bmatrix} \begin{Bmatrix} p_z^{(i+1)} \\ v_z^{(i+1)} \end{Bmatrix} \tag{3}$$

Where: $p_z^{(i)}$ is the sound pressure at the *i*-th end; $v_z^{(i)}$ is the normal velocity at the *i*-th end, Z_i is the equivalent characteristic impedance of the *i*-th layer, $Z_i = \rho_i c_i$.

Write equation (3) in the form of the following transfer matrix:

$$\boldsymbol{T}_i = \begin{bmatrix} \cos\, k_{iz} d_i & \mathrm{j} Z_i \sin\, k_{iz} d_i \\ \mathrm{j}\sin\, k_{iz} d_i / Z_i & \cos\, k_{iz} d_i \end{bmatrix} \tag{4}$$

According to the continuous conditions of pressure and vibration velocity at the interface of each layer, the transfer matrix is multiplied cumulatively to obtain the total transfer matrix in the following form:

$$\begin{Bmatrix} p_z^{(1)} \\ v_z^{(1)} \end{Bmatrix} = \boldsymbol{T}_1 \times \boldsymbol{T}_2 \times \cdots \times \boldsymbol{T}_n \begin{Bmatrix} p_z^{(n+1)} \\ v_z^{(n+1)} \end{Bmatrix} = \begin{bmatrix} T_{11} & T_{12} \\ T_{21} & T_{22} \end{bmatrix} \begin{Bmatrix} p_z^{(n+1)} \\ v_z^{(n+1)} \end{Bmatrix} \tag{5}$$

As a result, the input surface impedance Z_{in}, the complex reflection coefficient R, and the complex sound pressure transmission coefficientt_{p} of the equivalent multilayer homogeneous structure can be found respectively [7,11]:

$$Z_{\mathrm{in}} = \frac{p_z^{(1)}}{v_z^{(1)}}, R = \frac{Z_{\mathrm{in}} - Z_0}{Z_{\mathrm{in}} + Z_0}, t_{\mathrm{p}} = \frac{Z_{n+1}(1+R)}{T_{11} Z_{n+1} + T_{12}} \tag{6}$$

Only the effects of static pressure and cavity internal pressure on the structure are considered, the deformation and displacement are calculated by using finite element software. The deformation variables are imported into a two-dimensional theoretical model to calculate sound transmission loss (TL).

When the deformation of acoustic coatings under static pressure is obtained, the coatings unit with variable section containing the cylindrical cavity is divided into n layers. The inner diameters of the front and back interfaces of each layer are noted as $r_{bi,f}$ and $r_{bi,b}$, respectively. In particular, the average inner radius of each section of cylindrical cavity before deformation is:

$$r_{\mathrm{b}i} = (r_{\mathrm{b}i,\mathrm{f}} + r_{\mathrm{b}i,b})/2 \tag{7}$$

The cylindrical cavity of the coatings under static pressure is compressed internally, and the inner radius and thickness of its cavity unit structure are changed. Therefore, the average inner radius of each segment of cylindrical cavity unit structure after compression can be expressed as:

$$\overline{r}_{\mathrm{b}i} = [(r_{\mathrm{b}i,\mathrm{f}} + \Delta r_{\mathrm{b}i,\mathrm{f}}) + (r_{\mathrm{b}i,b} + \Delta r_{\mathrm{b}i,b})]/2 \tag{8}$$

where $\Delta r_{\mathrm{b}i,\mathrm{f}}$ and $\Delta r_{\mathrm{b}i,b}$ are the radial displacements of the inner diameter nodes at the front and rear interfaces of the unit structure of the *i*-th layer, respectively.

The outer boundary of the unit structure of the coatings satisfies the radial constraint. That is, the radial displacement of the outer wall node is 0. Therefore, the aperture rate is calculated using the new inner diameter, and the equivalent wave number and average impedance of each layer of the cylindrical cavity are further obtained. In addition, the axial coordinates of the front and back interfaces of each layer of the cylindrical cavity are $d_{i,\mathrm{f}}$ and $d_{i,b}$, respectively, and the thicken ss of the unit structure of the *i*-th layer of the cylindrical cavity after being compressed is:

$$\overline{d}_i = (d_{i,\mathrm{f}} + \Delta d_{i,\mathrm{f}}) - (d_{i,b} + \Delta d_{i,b})) \tag{9}$$

where: $d_{i,\mathrm{f}}$ and $d_{i,b}$ are the axial displacements at the front and rear interfaces of the cylindrical cavity unit structure of the *i*-th level, respectively. $\Delta d_{i,\mathrm{f}}$ and $\Delta d_{i,b}$ are the axial coordinates at the front and rear interfaces of each segment of the cylindrical cavity unit structure, respectively. The average inner diameter of the cylindrical cavity unit structure in the cover layer and the thickness of the cylindrical cavity unit structure of the *i*-th layer in each section are substituted into Eq. 2-4. Eventually, the TL under different static pressures can be found.

2.3 Hydrostatic deformation

It is a complex problem to characterize the interaction between the rubber substrate and the air inside the cavity. In this study, the air inside the cavity is simplified as the pressure ΔP acting on the cavity wall. At this point, the cavity is pressurized before and after the relationship between the air and pressure in the cavity is expressed as follows [3, 12]:

$$\frac{p}{p_0} = \left(\frac{\rho}{\rho_0}\right)^{\gamma} = \left(\frac{V_0}{V_{\mathrm{cavity}}}\right)^{\gamma} \tag{10}$$

where: p_0, p are the pressure in the cavity before and after compression, respectively, p_0=1.01×10^5 Pa; ρ_0, ρ are the density of air in the cavity before and after compression, respectively; V_0, V are the volumes of the cavities before and

after compression, respectively; γ is the gas constant, γ=1.4.

The air inside the cavity is squeezed, generating a pressure ΔP against the cavity wall and acting on the surface of the cavity, when the surface of the rubber substrate is subjected to hydrostatic pressure. The pressure ΔP against the cavity wall can be calculated by Eq. 11.

$$\Delta P = p - p_0 = p_0[(\frac{V_0}{V_{\text{cavity}}})^{\gamma} - 1] \tag{11}$$

The volume fraction cannot be calculated for cavity domains with undefined physical fields, in the hydrostatic calculations using COMSOL software. Since the cavity volume cannot be calculated using conventional methods, the Stokes formula is used to convert the volume into an area fraction on the boundary surface:

$$\oint (\nabla \cdot \xi) \mathrm{d}V = \oint \xi \cdot \mathrm{d}S \tag{12}$$

where: ∇ is the gradient operator; ξ is a particular function; S is the boundary surface of the domain V to be integrated.

After conversion, the volume of the cavity can be calculated as [13, 14]:

$$V_{cavity} = \oint_{V_{caxiy}} 1dV = -\oint_{V_{caily}} \left(\nabla \cdot \begin{bmatrix} 0 \\ 0 \\ z \end{bmatrix}\right) dV = \oint_{S_{caxiy}} (-z) \cdot n_z \, dS \tag{13}$$

Where: z is the z-directional coordinate of the point inside the cavity; n_z is the normal vector of z-directional coordinates; S_{cavity} is the wall surface inside the cavity. After the volume of the compressed cavity is obtained, ΔP can be defined as a variable in COMSOL, which acts as an external load on the cavity walls. Figure 6 shows a schematic diagram for calculating the deformation of the cover unit under static compression in COMSOL.

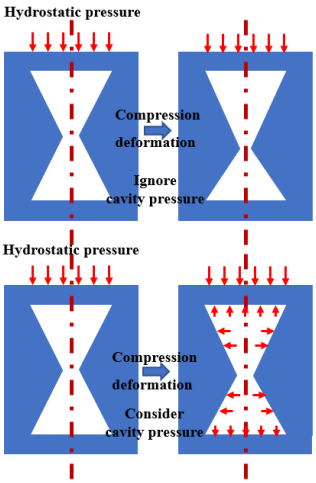

Figure 4. COMSOL calculation of deformation of anechoic coating unit cell under hydrostatic pressure.

It is worth noting that the single cell remains as a rotary body after deformation under the action of static and cavity pressures, so the subsequent calculations can continue to be performed using the two-dimensional axisymmetric mode.

2.4 Acoustic finite element model

The literature verified that a two-dimensional axisymmetric model can be used in calculating the acoustic properties of an infinite cover, and the finite element model is shown in Fig. 5.

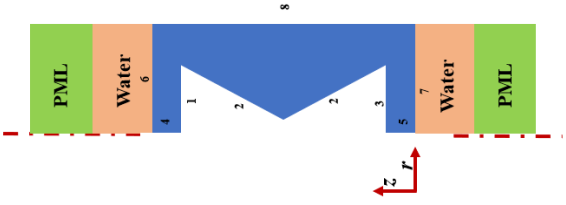

Figure 5. Two-dimensional axi-symmetric finite element models of acoustic coatings unit cell.

The z-axis is the rotation center axis of the model, and both the upper and lower interfaces of the acoustic coatings are connected to the water area. The sound wave is incident vertically from the upper end of the upper water area along the negative direction of the z-axis, the medium inside the cavity is set to be air or none, and the perfectly matched layer (PML: Perfectly matched layer) is set outside the upper and lower water areas. The acoustic coatings boundaries 1, 2 & 3 are the free boundary of the cavity; Boundary 4 & 5 are the axisymmetric boundary; the periodic boundary condition of the 3D model is transformed into the boundary with zero normal vector of the 2D axisymmetric model (boundary 8); the acoustic-solid coupling boundary (boundary 6 & 7) is set in the multi-physics field coupling to deal with the water-rubber coupling effect. In the finite element simulation, the " Acoustic-Solid Coupling" module is used, and the air inside the cavity and the water above and below the model are set as the "Pressure Acoustics" module, and the rubber material is set as the "Solid Mechanics "module. In particular, when the pressure in the cavity is considered, the contact surface of air and rubber should also be set to the "Acoustic-Solid Coupling" boundary [8-9].

By definition the sound insulation TL (sound transmission loss) can be expressed as [3,10]:

$$TL = 10log_{10}\frac{E_i}{E_t} \tag{14}$$

where E_i is the incident acoustic energy and E_t is the transmitted acoustic energy. Thecoatingswork at tens or even hundreds of meters underwater. The high-pressure environment will cause the dynamic mechanical properties of the cavity structure and materials of the coatings to change, and the resonance of the cavity will be suppressed, thus reducing the sound insulation performance. At the same time, the deformation of the coatings structure under hydrostatic pressure is irregular. Even if the deformation of the coatings under different hydrostatic pressures is obtained through structural mechanical analysis, it is difficult to match the actual cavity deformation in secondary modeling, which brings certain errors to the subsequent acoustic performance analysis. Based on the above problems, this study uses the moving mesh technique to divide the mesh directly on the deformed model to avoid the trouble of inaccurate secondary modeling, thereby calculating the sound insulation performance of the coatings more accurately.

2.5 Experimental model

The hydroacoustic tube test system shown in Fig. 6 is a special equipment used for acoustic performance testing and evaluation of small sample models of hydroacoustic materials. The whole system contains three sets of different tube diameter test device, this paper selects ϕ120mm pulse tube system, tube length 10m, the test pressure range of the system is 0MPa-6MPa. Measurement under different pressure conditions, need to ensure the sealing of the hydroacoustic tube and the tightness of the measured model and the wall of the tube good premise, pumped into the high-pressure gas source to maintain the pressure, and through the pressure gauge to detect the pressure difference between the upper and lower waters of the measured material.

Figure 6. The hydroacoustic tube test system.

Figure 7 shows the schematic diagram of the sound insulation measurement. Incident sound waves are absorbed and reflected in the hydroacoustic tube. Two microphones are placed in front of and behind the test material to measure the sound pressure at the location, and the standing wave separation method is used to separate the incident wave from the reflected wave and thus obtain the transmission coefficient. The transmission coefficient is calculated by the following equation [3, 4]:

$$t_p = \frac{\sin(k \cdot s1) \cdot p3e^{jks\,2} - p4}{\sin(k \cdot s2) \cdot p1 - p2e^{-jks\,1}} e^{jk\,(L1+L2)}$$

$$TL = -20lg|t_p| \tag{15}$$

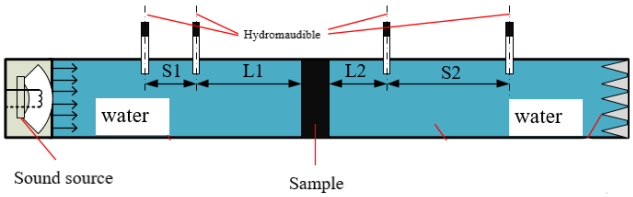

Figure 7. The schematic diagram of the sound insulation measurement.

3. Results and Discussion

The geometry of the acoustic coatings studied in this study is shown in Fig. 8. The corresponding samples prepared according to the geometry are sealed with a 5mm thick film below and above the sample, with a total height of 50mm and a test tube diameter of 118mm.

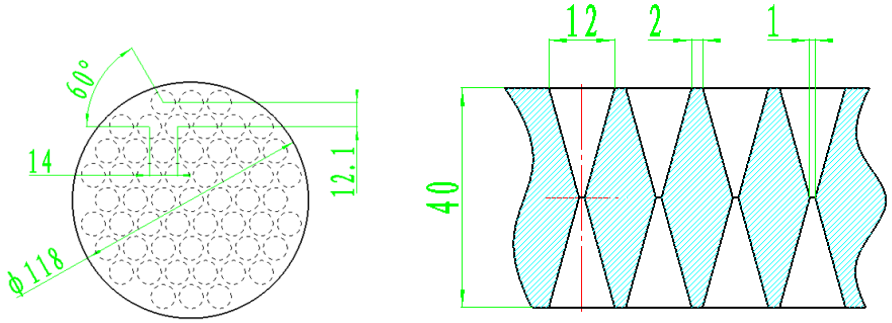

Figure 8. Schematic diagram of the size of the acoustic cavity structure.

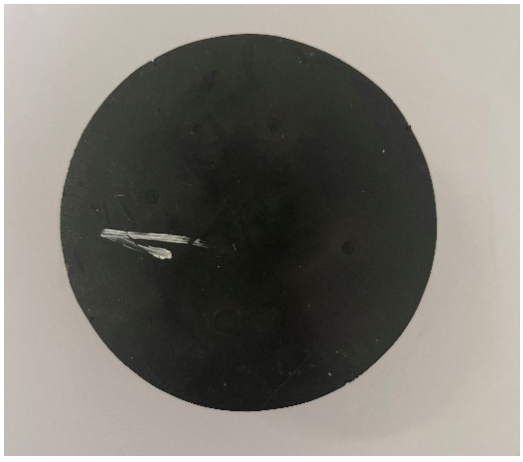

Figure 9. Physical drawing of sound tube test sample.

Rubber material parameters include Young's modulus, loss factor, Poisson's ratio, and density, where Poisson's ratio is 0.495 and density is 1.3 g/cm^3. Dynamic mechanical data of Young's modulus and loss factor (at 20℃) of this material are shown in Fig. 10:

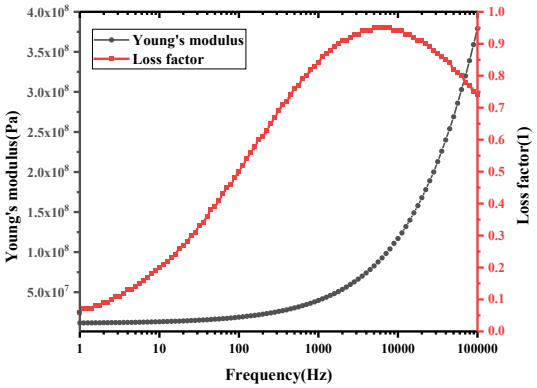

Figure 10. Rubber dynamic mechanical parameter curve.

Figure 11 shows the deformation displacement cloud diagram of the structure under the static load pressure of 1MPa and 3MPa.As can be seen from the figure, the radial and axial displacement of the single-cell model occurs under hydrostatic pressure, and its amplitude increases with the increase of pressure. It is worth noting that the air in the cavity has the effect of resisting structural deformation to a certain extent. Specifically, the maximum deformation at 1MPa is reduced by 0.1mm, and the maximum deformation at 3MPa is reduced by 0.5mm.

After calculating the static deformation of the structure, it is assumed that part of the model is still a cylindrical cavity. Substituted the geometric parameters of the length shortening radial contraction into the program to calculate the TL of the coatings. Finally, the deformation models are introduced into the finite element "Acoustic-Solid coupling" module to calculate the TL.

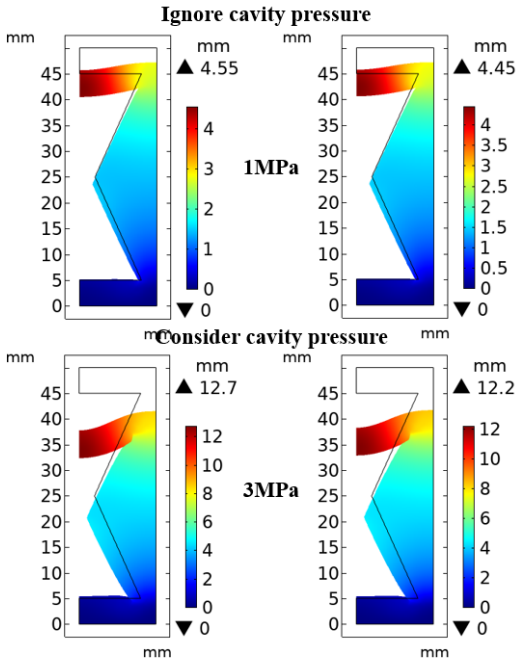

Figure 11. The displacement cloud diagrams under different working conditions.

The results of the finite element method (FEM) and the transfer matrix theory (TMT) are shown in Fig. 12. It should be noted that FEM(Y) represents the consideration of the internal pressure in the cavity, and on the contrary, FEM(N) is not considered. The results of the TMT and FEM calculations basically match when only the deformation is considered without considering the parameter changes of the rubber material under static pressure, which effectively illustrates the

accuracy of the TMT method for calculating the acoustic cover sound insulation performance under different pressures. It is worth noting that the acoustic cover layer deforms under static pressure, and the cavity pressure plays a role in resisting the shrinkage deformation under static pressure. When the static pressure is 0 MPa (Fig. 12), the cavity has no static pressure deformation and does not produce the corresponding resistance reaction force, at this time, the curves of sound absorption coefficients in the two cases of considering cavity pressure and no cavity pressure appear to overlap. However, with the increase of static pressure, the cavity is squeezed and the cavity pressure effect starts to be obvious.

The two calculated curves of FEM(Y) and FEM(N) show a deviation trend. Interestingly, the FEM(Y) curve is slightly lower than FEM(N), which indicates that the coupling of rubber and air contributes to the passage of acoustic waves.

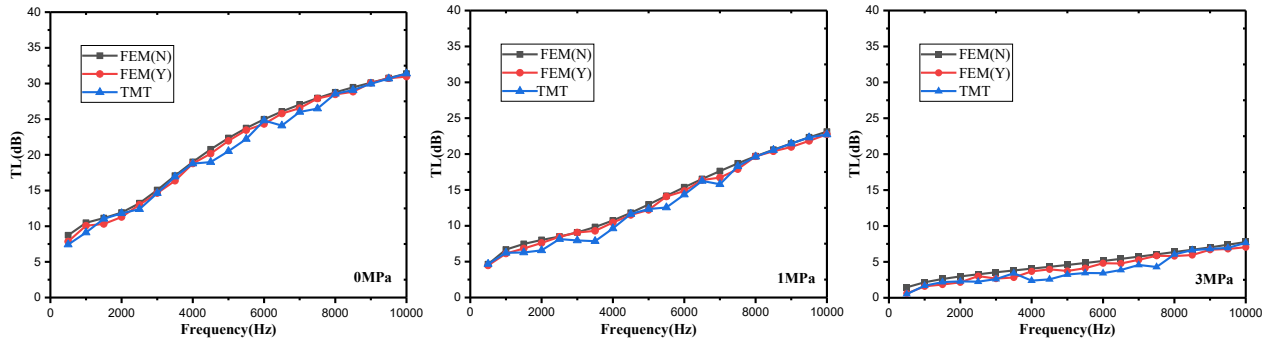

Figure 12. Comparison of TL of acoustic coatings with and without considering cavity pressure under different hydrostatic pressures.

Further, the experimental results show that the experimental test results and the finite element calculation results are basically consistent in numerical values with the same trend. It can be inferred that the theoretical model of this paper is correct with the finite element simulation model. It should be noted that the experimental results are lower than the simulation calculation results, and the reasons for this phenomenon are: (1) the mechanical parameters of the rubber material will change under different pressure conditions in the actual application, and the finite element simulation process does not consider the change; (2) the implementation of the non-reflective end of the experimental test process is different from the settings in the software; (3) the acoustic-solid coupling between the hydroacoustic pipe wall and the coatings and water in the experimental process is not considered in the simulation process.

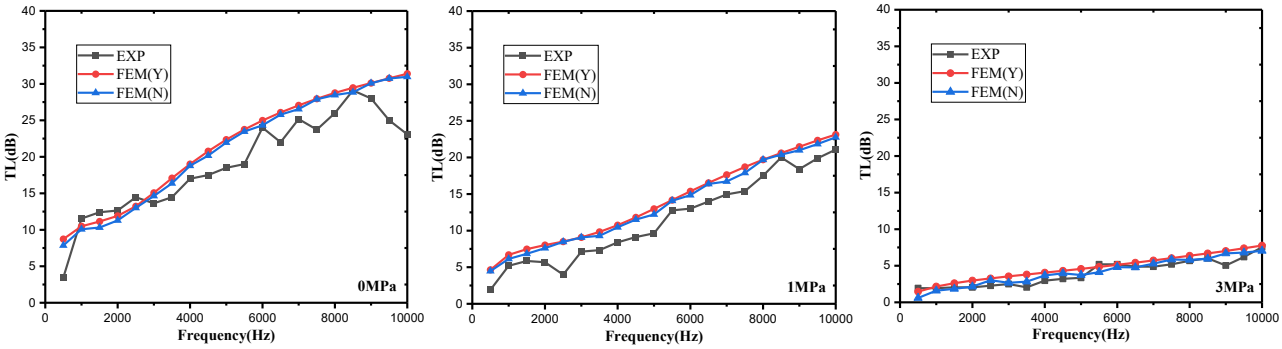

Figure 13. Comparison of numerical curves of FEM and EXP.

4. Conclusion

In this paper, the acoustic insulation performance of acoustic coverings containing cavities under static pressure is calculated and analyzed by theoretical analysis and finite element method, respectively, with an emphasis on the effect of cover deformation on the acoustic insulation performance under static pressure. Further, the applicability of the two-dimensional theory for calculating the acoustic coatings' sound insulation performance under static pressure is verified by calculation and experiment, which provides a reliable path for fast prediction of the sound insulation performance. Based on the research and experiments, the main conclusions are obtained as follows:

(1) If the change of rubber material parameters is not considered, the cavity of the acoustic coatings under static pressure will undergo axial and radial compression deformation. With the increase of static pressure, the sound insulation curve decays downward as a whole. In particular, when the deformation of the model under static pressure completely

destroys the acoustic coatings structure of the model, the acoustic properties of the acoustic coatings are almost completely lost.

(2) The cavity is compressively deformed under static pressure, and the air inside the cavity will generate cavity pressure under the structural deformation to resist the contraction deformation under the action of water pressure. When the static pressure is small, for the sound insulation coefficient curves obtained in the two cases of considering cavity pressure and no cavity pressure, the two basically overlap, and the curve considering cavity pressure is closer to the actual value. However, as the static pressure increases, the cavity structure deformation becomes obvious, and the cavity pressure effect starts to become weaker.

(3) Most of the current theoretical methods to analytically calculate the absorption coefficients of acoustic coverings decompose the cavity-containing underwater coatings into vacuum cylindrical cavities, which cannot consider the coupling effect of the air-rubber matrix inside the cavity, while the finite element method can achieve it. The results show that the theoretical method can effectively predict the sound insulation characteristics of acoustic coatings under different pressure conditions.

The proposed results show that the theoretical method can effectively predict the acoustic insulation characteristics of acoustic coatings under different pressure conditions. In summary, this work only considered the compressive deformation of the submerged acoustic coatings under static pressure and failed to consider the effect of material parameter changes on the sound insulation effect under static pressure. If the static and dynamic experimental parameters of rubber under static pressure are available in the subsequent study, they can be introduced into the deformation calculation and sound absorption calculation respectively according to the method of this paper, so as to obtain the acoustic coatings sound insulation performance closer to the actual one.

References

[1] Gaunaurd, G. (1997). One-dimensional model for acoustic absorption in a viscoelastic medium containing short cylindrical cavities. *The Journal of the Acoustical Society of America*, 62(2): 298–307.

[2] Zhu, B.L. and Huang, X.C. (2014). Technology of Submarine Acoustic Stealth: Design of Acoustic Coating. *Shanghai Jiao Tong University Press*. (in Chinese)

[3] Ervennka, P. and Challande, P. (1991). A new efficient algorithm to compute the exact reflection and transmission factors for plane waves in layered absorbing media (liquids and solids). *The Journal of the Acoustical Society of America*, 89(4): 1579–1589.

[4] Jiang, W. W., Cheng, Y., Zhu, Y. (2006). Computation and analysis of sound absorption performance of rubber structures under variable hydraulic pressure. *Noise and Vibration Control*, 26(5): 55–57, 73. (in Chinese)

[5] Huang, X. C., Zhu, B. L., Hu, P., et al. (2013). Measurement of dynamic properties of rubber under hydrostatic pressure by water-filled acoustic tube. *Journal of Shanghai Jiao Tong University*, 47(10): 1503–1508, 1519. (in Chinese)

[6] Brunner, D., Junge, M., Gaul, L. (2009). A comparison of FE-BE coupling schemes for large-scale problems with fluid structure interaction. *International Journal for Numerical Methods in Engineering*, 77(5): 664-688.

[7] Wang, S., Hu, B., Li, S., et al. (2022). Acoustic performance of cavities with gradient changes of cavity numbers under low lattice constant in a soft elastic medium. *Noise Control Engineering Journal*, (3):70.

[8] Tao, M. and Jiang, K. (2016). Dynamic parameters measurement of damping materials under hydrostatic pressure based on a hybrid numerical-analytical method. *Journal of Vibration and Shock*, 35(7): 96–101. (in Chinese)

[9] Ye, C. Z, Liu, X. W., Xin, F. X., et al. (2018). Influence of hole shape on sound absorption of underwater anechoic layers. *Journal of Sound and Vibration*, 426: 54–74.

[10] Shi, K., Jin, G., Ye, T., et al. (2019). Underwater sound absorption characteristics of metamaterials with steel plate backing**.** *Applied Acoustics*, 153(OCT.):147-156.

[11] Fang, Z. and Liu, C. Y. (2017). Combined mesh free method and mode matching approach for transmission loss predictions of expansion chamber silencers. *Engineering Analysis with Boundary Elements*, 84: 168.

[12] Zhu, H. A., Zhang, D. Y., Zhang, W.T., et al. (2021). Real-time monitoring of airborne molecular contamination on antireflection silica coatings using surface acoustic wave technology. *Sensors and Actuators, A. Physical.* 329(1).

[13] Ke, Y., Zhang, L., Zhao, X., et al. (2021). An equivalent method for predicting acoustic scattering of coated shell using identified viscoelastic parameters of anechoic coating. *Applied Acoustics*, 33 (4): 335-447.

[14] Zou, M. S., Jiang. L. W., Liu. S. X. (2018). Underwater acoustic radiation by structures arbitrarily covered with acoustic coatings. *Journal of Sound and Vibration*, 17(3): 56-65.